Heliyon 10 (2024) e29427

Contents lists available at ScienceDirect

Heliyon

journal homepage: www.cell.com/heliyon

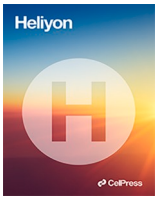

Research article

Revealing the role of material properties in impact-related injuries: Investigating the influence of brain and skull density variations on head injury severity

Hamed Abdi [a,*], David Sánchez-Molina [b,**], Silvia García-Vilana [b], Vafa Rahimi-Movaghar [a]

[a] Sina Trauma and Surgery Research Center, Tehran University of Medical Sciences, Tehran, Iran
[b] Universitat Politècnica de Catalunya, GIES, Av. Eduard Maristany, 16, 08019 Barcelona, Spain

ARTICLE INFO

Keywords:
Traumatic brain injuries (TBI)
Finite element model (FEM)
Density
Viscoelastic materials
Head impact
Head injury criterion (HIC)
Injury prevention

ABSTRACT

Traumatic brain injuries (TBI) resulting from head impacts are a major public health concern, which prompted our research to investigate the complex relationship between the material properties of brain tissue and the severity of TBI. The goal of this research is to investigate how variations in brain and skull density influence the vulnerability of brain tissue to traumatic injury, thereby enhancing our understanding of injury mechanism.

To achieve this goal, we employed a well-validated finite element head model (FEHM). The current investigation was divided into two phases: in the first one, three distinct brain viscoelastic materials that had been utilized in prior studies were analyzed. The review of the properties of these three materials has been meticulous, encompassing both the spectrum of mechanical properties and the behaviors that are relevant to the way in which brain tissue reacts to traumatic loading conditions. In the second phase, the material properties of both the brain and skull tissue, alongside the impact conditions, were held constant. After this step, the focus was directed towards the variation of density in the brain and skull, which was consistent with the results obtained from previous experimental investigations, in order to determine the precise impact of these variations in density. This approach allowed a more profound comprehension of the impacts that density had on the simulation results.

In the first phase, Material No. 2 exhibited the highest maximum first principal strain value in the frontal region (ε_{max} = 15.41%), indicating lower stiffness to instantaneous deformation. This characteristic suggests that Material No. 2 may deform more extensively upon impact, potentially increasing the risk of injury due to its viscoelastic behavior. In contrast, Material No. 1, with a lower maximum first principal strain in the frontal region (ε_{max} = 7.87%), displayed greater stiffness to instantaneous deformation, potentially reducing the risk of brain injury upon head impact. The second phase provided quantitative findings revealing a proportional relationship between brain tissue density and the pressures experienced by the brain. A 2 % increase in brain tissue density corresponded to approximately a 1 % increase in pressure on the brain tissue. Similarly, changes in skull density exhibited a similar quantitative relationship, with a 6 % increase in skull density leading to a 2.5 % increase in brain pressure. This preliminary approximate ratio of 2 to 1 between brain and skull density variations provides an initial quantitative

* Corresponding author.
** Corresponding author. David Sánchez-Molina
E-mail addresses: h-abdi@farabi.tums.ac.ir (H. Abdi), david.sanchez-molina@upc.edu (D. Sánchez-Molina).

https://doi.org/10.1016/j.heliyon.2024.e29427
Received 13 November 2023; Received in revised form 5 April 2024; Accepted 8 April 2024
Available online 9 April 2024

framework for assessing the impact of density changes on brain vulnerability. These findings have several implications for the development of protective measures and injury prevention strategies, particularly in contexts where head trauma is a major issue.

1. Introduction

Head injuries caused by impacts, such as those encountered in sports, automobile collisions, or other traumatic occurrences, remain a substantial issue in the fields of public health and medical investigation [1–3]. An estimated 69 million individuals worldwide are affected by traumatic brain injury (TBI) on an annual basis [4]. These injuries can vary in severity, spanning from minor concussions to more severe and potentially life-threatening conditions [5]. The investigation of the complex interrelationships among various elements that contribute to the severity of head injuries is a critical undertaking with the capacity to enhance our knowledge of injury mechanics and direct the creation of more effective preventative and therapeutic approaches [6–12]. A critical aspect of this interplay is the relationship between the material properties of the human brain and the resulting impact-related injury outcomes [13–15]. Despite significant progress in the comprehension of the mechanisms underlying head injuries, there remains a knowledge gap regarding the exact impact that properties of brain material have on the severity of such injuries. Although the influence of impact force, angle, and velocity on resulting injuries is widely recognized, the intricate impact of variations in brain density and other material properties has received relatively less attention in the scientific literature [3,16–20]. Addressing this gap is essential to improve our prediction and to develop effective countermeasures to mitigate the consequences of head impacts.

Over the years, significant strides have been made in the realm of biomechanics through the development of intricate human head models or FEHMs. Prominent examples of FEHMs include: WSUBIM, KTH head model, UCDBTM, Bin Yang model, WHIM, and YEAHM [21–26]. These models have played a crucial role in simulating head biomechanics, aiding in the understanding of injury mechanisms and guiding prevention strategies. Ongoing efforts in the scientific community are dedicated to refining these FEHMs improving their accuracy and reliability [27,28]. On the other hand, the chosen material models for simulating various finite element models hold pivotal significance in comprehending the mechanical reactions to external loads. Biomechanically, the precise material properties inherent in the human brain are undergoing meticulous investigation [29–31]. Extensive research has been conducted on cadaver and animal brains for several decades. It is important to note that brain tissue properties tend to change after blood circulation ceases; thus, the complete mechanical profile of the brain in a living human remains somewhat speculative. Additionally, the material properties used in these models are mainly in the direction of using viscoelastic models [32,33]. Despite these advancements, there is a persistent pursuit of material properties that closely mimic human head tissues, ensuring a more accurate representation of real-world scenarios [34].

This study delves into the intricate connection between brain tissue material properties and head injury severity, focusing on the variations in brain and skull density to quantitatively investigate the influence of these variations on injury outcomes. By shedding light on the nuanced relationship between these material properties and their contribution to injury severity, we provide valuable insights that inform the design of more targeted protective strategies and better medical interventions. To achieve this, we employ advanced computational models, experimental data, and sophisticated analytical techniques to unravel the complex mechanisms that underlie impact-related head injuries.

2. Materials and methods

2.1. Study design

The study included a comprehensive comparative analysis that examined three distinct brain viscoelastic materials utilized in previous research. A comprehensive literature review was conducted on these materials, covering a wide range of mechanical properties and behaviors that are relevant to the way in which brain tissue reacts to traumatic loading conditions. To address the objectives of the present research, a well-established validated FEHM was employed for computational biomechanics analysis. Then, using this FEHM, each brain material was simulated with an identical impact scenario.

In the subsequent phase, the material properties of both the brain and skull tissue, alongside the impact conditions, were held constant. The focus then shifted to the manipulation of brain and skull density—aligning with findings from existing experimental studies—to ascertain the specific influence of density variations. This approach allowed for a deeper understanding of the effects of density on the simulation results.

The starting hypotheses is that cranial density will alter the mass of the skull, which would affect both frontal and occipital principal strain stresses. It is also expected that internal pressure would be affected by the viscoelastic properties of the brain tissue.

2.2. Brain material properties

Comprehending the strain-rate-dependent behavior of brain tissues is critical owing to the intricate characteristics of TBI. Consequently, viscoelastic models are preferentially utilized when determining the mechanical property values for simulating the mechanical behavior of the brain [33,35,36]. The shear modulus for a viscoelastic tissue in the brain can be expressed as follows:

$$G(t) = G_\infty + (G_0 - G_\infty)e^{-\beta t}$$

Here, G_0 represents the short-term shear modulus, G_∞ signifies the long-term shear modulus, β stands for the relaxation constant, and t corresponds to the time after a stress increase.

In this study, we examined three distinct groups of viscoelastic brain materials carefully chosen from well-established literature sources to encompass a diverse spectrum of mechanical characteristics [24,37–39]. The detailed properties of these three groups are summarized in Table 1.

In the study conducted by Wenyi Yan et al. [39], the long-term elastic modulus, bulk modulus, and Poisson's ratio were documented as 22.8 kPa, 2.278 GPa, and 0.499991, respectively. Delving into the domain of viscoelasticity, the relaxation shear modulus $G_R(t)$ is governed by a dimensionless function, $g_R(t)$, expressed as a Prony series:

$$g_{R^{(t)}} = 1 - 0.8150 \times \left(1 - e^{-t/0.00143}\right)$$

$$g_R(t) = G_R(t)/G_0$$

This function captures the intricate interplay of strain-rate-dependent properties in the material response. G_∞ can be obtained from the Prony series for the time $t \to \infty$, as:

$$G_\infty = G_R(\infty) = g_R(\infty) \times G_0$$

In the present study, these three groups of materials were defined using the Prony series in COMSOL Multiphysics software.

2.3. Brain and skull density variations across previous studies

Variations in tissue density lead to changes in mass, potentially influencing the numerical outcomes in simulations of head injuries. Consequently, it is critical to examine the density parameters utilized in numerous biomechanical investigations of head trauma. In this context, we undertook a comprehensive examination of brain and skull bone tissue densities across diverse previous investigations. A review of the range of brain tissue densities in the scientific literature shows that the lowest density measured in these studies was 1040 kg/m^3 [39]. At the other end of the range, the highest brain tissue density used was 1140 kg/m^3 [40]. In terms of skull bone density, the studies by Horgan et al. [38] and Kleiven et al. [22] and Yan et al. [39] used the lowest density value at 2000 kg/m^3. On the upper scale, the highest skull density value was noted at 2120 kg/m^3 [41]. In order to provide a comprehensive summary of the specific brain and skull tissue density values utilized in diverse biomechanical simulations of head trauma, refer to Table 2.

The comprehensive analysis of tissue density variations across these studies facilitates a deeper understanding of the range of parameters considered in biomechanics studies related to head trauma.

2.4. Finite element head model and impact conditions

The FEHM utilized in this study was meticulously constructed and rigorously validated in our prior research endeavor [43]. This comprehensive model was developed by leveraging computed tomography (CT) scan and magnetic resonance imaging (MRI) techniques acquired from a 36-year-old individual, ensuring a robust foundation for subsequent simulations. The intricacies of the model encompassed the scalp, skull, cerebrospinal fluid (CSF), and brain, collectively providing a holistic representation of the complex head-brain system.

For the simulation of head impact dynamics, we turned to COMSOL Multiphysics, a powerful finite element analysis software package renowned for its ability to handle coupled physical phenomena across diverse domains, including fluid dynamics and structural mechanics. In our study, we utilized COMSOL's capabilities to execute a fluid-structure interaction (FSI) model. This approach allowed us to accurately replicate the intricate interactions between the CSF and surrounding structures during head impact scenarios.

Within our FSI model, the CSF was conceptualized as a fluid domain with specific properties, including a density of 1000 kg/m^3 and a dynamic viscosity of 0.001 Pa *s*. Meanwhile, neighboring structures such as the skull bones, facial bones, and brain tissue were represented as solid domains. COMSOL Multiphysics facilitated the seamless integration of these fluid and solid domains, enabling us to capture the complex interplay between the CSF dynamics and the mechanical response of the surrounding tissues during head impact simulations.

The material properties of skull and facial bones were considered elastic, and brain tissue was viscoelastic. The density, Young's modulus and Poisson's ratio of the facial bones are 1060 kg/m^3, 500 MPa and 0.22, respectively. The material properties of skull bone and brain tissue are shown in Tables 1 and 2

Table 1
Mechanical properties of viscoelastic brain material groups.

Material No.	Research Group	Density (kg/m^3)	Shear Modulus G_0 (kPa)	Shear Modulus G_∞ (kPa)	Decay constant (s^{-1})	Bulk Modulus (GPa)
1	Zhang - Bin Yang	1040	41	7.8	700	2.19
2	Horgan	1060	12.5	2.5	80	2.19
3	Wenyi Yan	1040	–	–	700	2.278

Table 2
Brain and skull density variations in biomechanical studies.

Study	Publication date	Brain Tissue Density (kg/m3)	Skull Bone Density (kg/m3)	References
Willinger	1999	1140	2100	[40]
Horgan	2004	1060	2000	[38]
Kleiven	2007	1040	2000	[22]
Zoghi-Moghadam	2009	1040	2120	[41]
Ying Chen	2010	1040	2070	[42]
Wenyi Yan	2011	1040	2000	[39]

The current study focuses specifically on examining rotational loading in the sagittal plane, prompted by the prevalent observation of anterior-posterior head motion in frontal collisions. To address this pivotal facet, experimental kinematics was implemented, resulting in peaks of translational acceleration and rotational accelerations of 450 g and 26200 rad/s^2, respectively [44]. These acceleration curves, portraying the translation and rotation of the head, were derived from the extensive work conducted by Depreitere et al. (2006), recognized as a cornerstone in whole-body cadaver studies on bridging vein rupture. In Depreitere et al.'s experiments, human cadaver bodies assumed an upright sitting posture, with the back of the head exposed to a pendulum impact simulating a frontal collision. The study reported 18 impact tests, encompassing cases with bridging vein rupture, those without rupture, and artifacts. Maximum rotational and translational accelerations, along with pulse duration, were meticulously documented. Fig. 1 in our study provides an illustrative representation of acceleration pulses sourced from Depreitere et al.'s research, specifically capturing instances leading to cerebral bridging vein rupture. Widely acknowledged and employed in various studies, this figure ensures our study's reliance on robust experimental data from the referenced research.

The loading conditions utilized for impact are illustrated visually in Fig. 1. These conditions consist of translational motion along the z-axis and clockwise rotational motion along the x-axis. Two reference points were established, with one situated in the central frontal region and the other in the central occipital region. It is important to highlight that the consistent positioning of these points

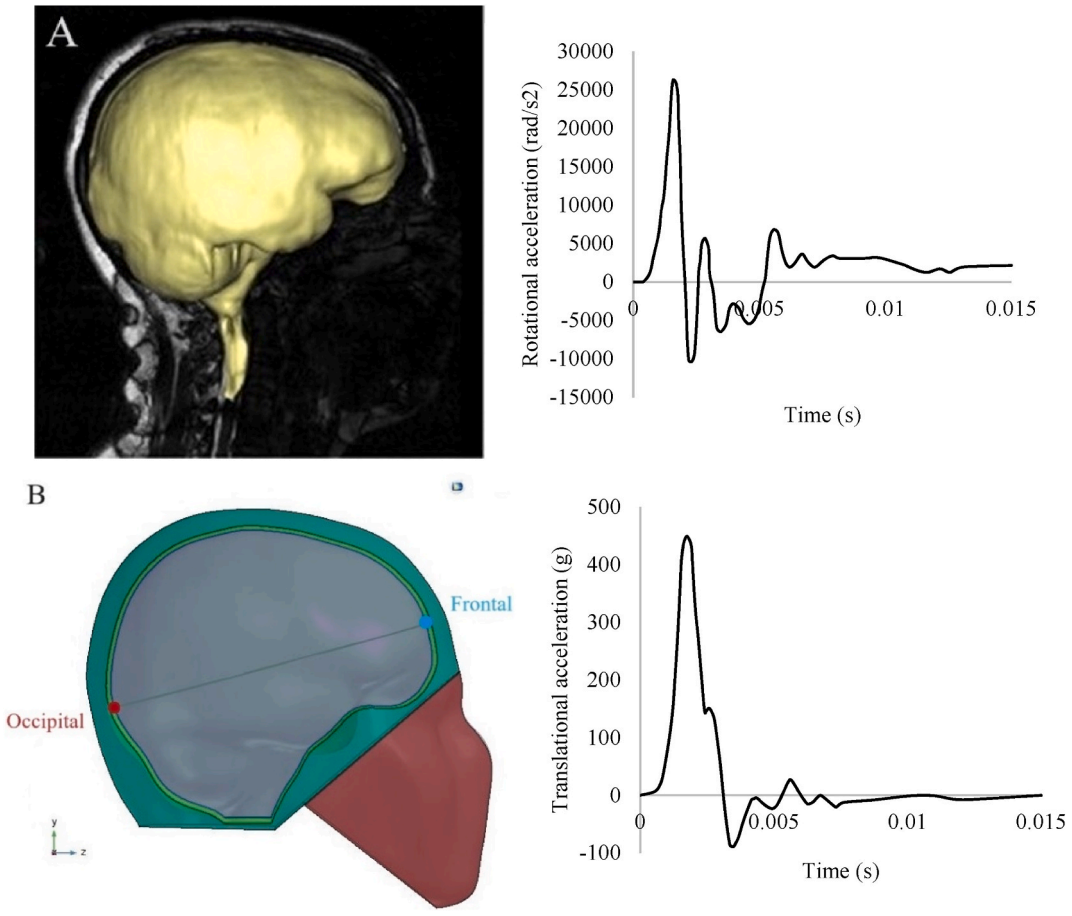

Fig. 1. Left: A: Head model B: Brain regions of interest for result extraction (frontal and occipital). Right: Head loading conditions employed in the impact study, showcasing rotational acceleration and translational acceleration.

across all models ensured uniformity. Subsequently, the outcomes and responses were derived from these specified regions, undergoing a thorough and comparative analysis. It is worth noting that while variations may naturally occur in results obtained from other locations, the uniformity of conditions in these analyses enhances the reliability and generalizability of the findings. Table 3 shows the results of mesh sensitivity analysis in the Wenyi Yan's study material group.

3. Results

This section presents a quantitative analysis of the outcomes obtained from various simulations subjected to head impact conditions. This comparative assessment aims to elucidate the differences in mechanical responses among these material groups within distinct regions of the brain.

3.1. Results of the viscoelastic brain material groups

The quantitative results from the three viscoelastic brain material groups are summarized in Table 4. The table presents the highest computed pressure values and the corresponding maximum first principal strain for both the frontal and occipital regions.

When the maximum pressure values of the material groups are compared, it is evident that material No. 2 exhibits the highest pressures on both the frontal and occipital regions (−260,077 and 213,641 Pa, respectively). This suggests that the material characteristics present in this group contributed to pressure distributions that were more intense during impact. On the contrary, Material No. 3 exhibits lower pressure values (−256,868 and 211,148 Pa, respectively), suggesting a potentially less severe biomechanical response. However, these changes were not noticeable. The percentage change from the lowest number to the highest number is approximately 1 %.

In terms of the maximum first principal strain, Material No. 2 exhibits the highest values for the frontal region (15.41 %), and material No. 3 exhibits the highest values for the occipital areas (12.65 %). This suggests that the material properties employed in Groups 2 and 3 contributed to relatively higher strains in response to the applied impact conditions. Conversely, Material No. 1 displays the lowest strain, signifying a comparatively more resilient material response. It is notable that in the frontal region, the percentage change from the smaller number (7.87 %) to the larger number (15.41 %) is approximately 96 %, and in the occipital region, it is approximately 52 %. These results were derived from the reference points defined in the central frontal and central occipital regions. However, it is noteworthy that the right and left frontal regions exhibited the highest strain levels. In contrast to brain pressure, which exhibited minimal changes, the variations in first principal strains were significant. Fig. 2 illustrates contours of brain pressure at time = 0.0017 s. In A-1, a sagittal view of the brain is presented using the material property from Zhang and Bin Yang's study. B-1 showcases results based on Horgan's study, while C-1 displays findings from Wenyi Yan's study. Furthermore, the contours of the first principal strain at time = 0.015 s are illustrated in the corresponding models (A-2, B-2, and C-2).

3.2. Results of brain and skull density variations

Table 5 presents the results derived from the brain and skull density variations utilized in the simulation, which includes twelve scenarios based on different density combinations. A detailed examination of the results reveals that simulation No. 1, characterized by the lowest density of both the brain and skull, exhibits the least amount of maximum pressure on the brain tissue in the frontal and occipital regions, recording values of −253285 Pa and 207986 Pa, respectively. Conversely, simulation No. 12, featuring the highest density of both the brain and skull, demonstrates the highest values. A comparative analysis between simulation No. 1 and No. 12 reveals increases of 8 % in brain pressure in both frontal and occipital regions.

In instances where the density of the brain was held constant at 1040 kg/m^3 and only the density of the skull bone was altered (simulations No. 1 to 4), a 1.8 % increase in brain pressure was observed for the frontal and occipital regions. Further investigation involving simulations No. 5 to 8, with a constant brain density of 1060 kg/m^3, as well as simulations No. 9 to 12, with a constant brain density of 1140 kg/m^3, respectively, 2.1 % and 2.6 % pressure increase was observed.

Fig. 3 illustrates the relationship between brain tissue density and occipital brain pressure across varying skull bone densities (2000 kg/m^3, 2070 kg/m^3, 2100 kg/m^3, and 2120 kg/m^3). Each series maintained a constant skull bone density level, allowing us to isolate the effect of brain tissue density on occipital brain pressure. Our analysis revealed consistent positive correlations, characterized by linear equations with specific slopes representing the rate of change in occipital brain pressure concerning changes in brain tissue density. Regardless of the skull bone density, increasing brain tissue density led to higher occipital brain pressure, reinforcing the robustness of this observed relationship.

Table 3
Mesh sensitivity results in the Wenyi Yan's study material group.

Run No.	1	2	3	4	5	6	7
Number of elements	7992	15805	28279	62638	80599	87014	95746
Frontal Pressure (Pa)	−255159	−255978	−254960	−255555	−256858	−256860	−256868

Table 4
Quantitative results of viscoelastic brain material groups.

Material No.	Maximum Pressure on frontal	Maximum Pressure on occipital	Maximum First Principal Strain on frontal	Maximum First Principal Strain on occipital
1	−258,076 Pa	211,638 Pa	7.87 %	8.31 %
2	−260,077 Pa	213,641 Pa	15.41 %	11.04 %
3	−256,868 Pa	211,148 Pa	14.43 %	12.65 %

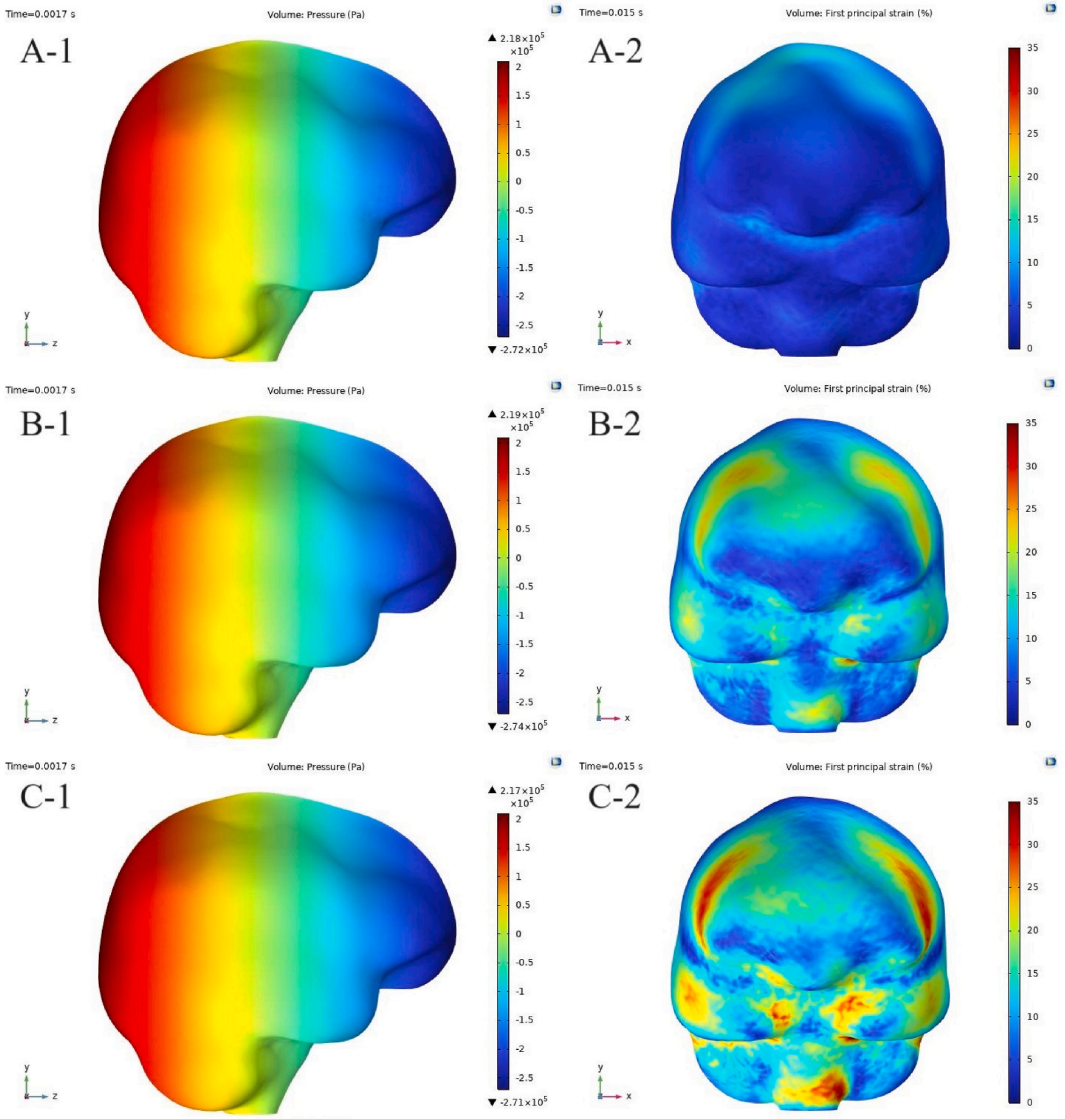

Fig. 2. Contours of brain pressure at time = 0.0017 s and first principal strain at time = 0.015 s in sagittal and frontal views, respectively. A-1, A-2: Sagittal and frontal views based on the material property of Zhang and Bin Yang's study. B-1, B-2: Sagittal and frontal views from Horgan's study. C-1, C-2: Sagittal and frontal views derived from Wenyi Yan's study.

4. Discussion

4.1. Viscoelastic brain material groups

In this phase of the study, we investigated the behavior of different materials in response to applied impact conditions, focusing on the maximum pressure and maximum first principal strain values in both the frontal and occipital regions of the brain. The analysis of

Table 5
Simulation results in the frontal and occipital regions of the brain at time = 0.0017 s.

Simulation No.	Brain Tissue Density (kg/m3)	Skull Bone Density (kg/m3)	Pressure (Pa) on Frontal	Maximum Pressure (Pa) on Occipital	Maximum First Principal Strain (%) on Frontal	Maximum First Principal Strain (%) on Occipital
1	1040	2000	−253285	207986	13.25	10.69
2	1040	2070	−255464	209903	13.46	10.89
3	1040	2100	−256905	211051	13.56	10.99
4	1040	2120	−257852	211801	13.63	11.05
5	1060	2000	−255677	210045	13.36	10.67
6	1060	2070	−258582	212437	13.60	10.90
7	1060	2100	−260066	213615	13.68	10.96
8	1060	2120	−261068	214426	13.78	11.04
9	1140	2000	−266387	218799	13.71	10.53
10	1140	2070	−270484	222347	13.96	10.77
11	1140	2100	−272126	223674	14.05	10.84
12	1140	2120	−273189	224532	13.92	10.75

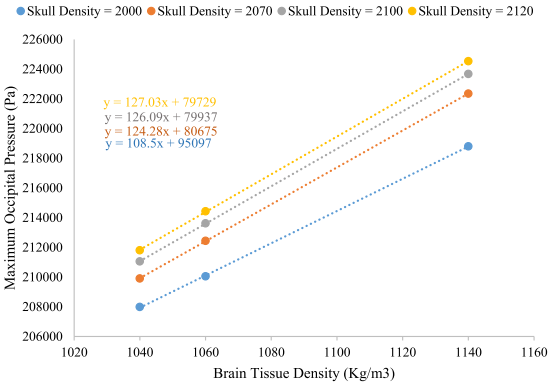

Fig. 3. The relationship between brain tissue density and occipital brain pressure at constant levels of skull bone density.

the maximum first principal strain revealed significant variations in the material response, which can be attributed to the inherent properties of the materials.

TBI is a complex and serious medical condition that can result from external forces applied to the head [12,17,20,22]. In cases of TBI, it is critical to assess how materials respond to these forces, considering both instantaneous deformation and time-dependent responses. This is where viscoelastic materials come into play, as they can accurately represent the mechanical behavior of brain tissue, which is viscoelastic in nature. Viscoelastic materials, such as those employed in our study, encompass both elastic and viscous properties. The elastic component enables them to store and release energy, which is vital for absorbing and dissipating impact energy. The viscous component accounts for time-dependent deformation and stress relaxation, a crucial factor when modeling TBI scenarios, where the brain tissue may continue to deform gradually over time following an impact. Our results reveal significant differences in the materials' response to head impacts, taking into account their viscoelastic properties. Material No. 2 exhibits the highest maximum first principal strain value in the frontal region (15.41 %), signifying its lower resilience concerning instantaneous deformation. In the context of TBI, this could suggest that Material No. 2 may exhibit a more pronounced deformation upon impact, potentially increasing the risk of injury due to the prolonged deformation associated with its viscoelastic behavior. Conversely, Material No. 1, with its lower maximum first principal strain in the frontal region (7.87 %), demonstrates a more resilient response regarding instantaneous deformation. This characteristic could be advantageous in mitigating TBI risk, as it suggests that Material No. 1 undergoes minimal deformation upon head impact, limiting the potential for brain injury. Material No. 3 falls in between, displaying an intermediate viscoelastic response in the frontal region with a maximum first principal strain of 14.43 %. In the occipital region, the results also provide insights into the viscoelastic behavior of materials and its implications for TBI. Material No. 3 shows the highest strain values, indicating a less resilient response (12.65 %). Material No. 2 displays intermediate values (11.04 %), while Material No. 1 exhibits the lowest strain (8.31 %). These findings underscore the complex nature of TBI, where the response of brain tissue to impacts in different regions of the head can vary significantly. The percentage change from the lowest to the highest strain values in both regions, when considering the viscoelastic properties, emphasizes not only the immediate deformation but also the continued deformation over time. This aspect is of critical importance in TBI scenarios, where the prolonged deformation of brain tissue can contribute to injury severity.

4.2. Brain and skull density variations

The results of this study offer significant quantitative insights into the potential relationship between brain and skull density variations and their implications for brain tissue vulnerability to traumatic injury. In our controlled simulations, we examined the effects of altering the density of both brain tissue and skull bone while keeping all other parameters consistent. These findings hold substantial implications for the fields of biomechanics and injury prevention.

The results suggest a possible quantitative association between brain tissue density and the pressures experienced by brain tissue during mechanical impacts. When we increased the brain tissue density by approximately 2 % from the baseline density of 1040 kg/m^3 to 1060 kg/m^3, we observed a proportional increase in pressure on the brain tissue. Specifically, this change in density led to an approximate 1 % increase in pressure on the brain tissue. These findings underline the potential quantitative role of brain tissue density in determining vulnerability to injury. In parallel investigations, we explored the effects of altering skull bone density while maintaining consistent simulation parameters. Increasing skull density by approximately 6 % from 2000 kg/m^3 to 2120 kg/m^3 appeared to result in a 1.8–2.5 % increase in pressure on the brain tissue. These quantitative findings suggest that the skull's density can significantly impact the forces transmitted to the brain during impacts. A possible quantitative ratio of 2 to 1 has been observed within this range of density variations, providing an initial quantitative framework for assessing the relationship between density changes and brain vulnerability. These initial quantitative observations have potential implications for the development of protective measures and injury prevention strategies in contexts where head trauma is a concern.

4.3. Limitations

While the current study provides valuable insights into the biomechanical responses under head impact conditions, several limitations need to be acknowledged. These limitations may impact the generalizability and applicability of the findings.

- Simplified Simulation Conditions: The simulation conditions utilized in this study, although carefully designed, inherently simplify the complex nature of real-world head impacts. The biomechanical responses observed in simulations might not comprehensively represent the complex dynamics and variations that occur during real-life traumatic events.
- Sensitivity to Material Properties: The study primarily focused on variations in material density, overlooking potential interactions with other mechanical parameters. It is acknowledged that changes in the density of a tissue can influence other material properties. While density variations were isolated to demonstrate their impact, assuming other parameters to be constant is a simplification. Future studies should explore the comprehensive interplay of material properties to provide a more nuanced understanding of the biomechanical response to head impacts.
- Limited Material Diversity: The study focused on three viscoelastic brain material groups, potentially limiting the generalizability of the results to a broader range of materials with varying mechanical properties. Including a more diverse set of materials in future studies would enhance the understanding of how different materials respond to head impact conditions.

5. Conclusion

The present investigation explored the complex relationship between brain and skull density variations and their impact on brain tissue vulnerability to traumatic injury. We acquired significant insights through the utilization of a validated finite element head model and a two-phase investigation. The main phase of study unveiled a direct correlation between brain and skull density and the pressures experienced by the brain. A 2 % increase in brain tissue density resulted in approximately a 1 % increase in brain tissue pressure, while a 6 % increase in skull density led to a 2.5 % increase in brain pressure. This approximate 2 to 1 ratio between brain and skull density variations provides a quantitative framework for assessing brain vulnerability due to density changes. In our ongoing effort to improve preventive measures and protective strategies, these findings establish a fundamental basis for further investigations that will contribute our comprehension of head injury biomechanics.

Data availability statement

Due to the restrictions imposed by the legal collaboration agreement between IMLFC and UPC, the data are not publicly available, although they can be accessed upon non-anonymous request to the authors of the study and under the conditions set by the aforementioned legal collaboration agreement.

CRediT authorship contribution statement

Hamed Abdi: Writing – review & editing, Writing – original draft, Visualization, Validation, Supervision, Software, Resources, Project administration, Methodology, Investigation, Funding acquisition, Formal analysis, Data curation, Conceptualization. **David Sánchez-Molina:** Writing – review & editing, Writing – original draft, Validation, Supervision, Methodology, Investigation, Conceptualization. **Silvia García-Vilana:** Writing – review & editing, Writing – original draft, Visualization, Supervision, Software, Methodology, Investigation, Conceptualization. **Vafa Rahimi-Movaghar:** Writing – review & editing, Writing – original draft, Supervision, Project administration, Investigation.

Declaration of competing interest

The authors declare that they have no known competing financial interests or personal relationships that could have appeared to influence the work reported in this paper.

References

[1] A. Brazinova, V. Rehorcikova, M.S. Taylor, et al., Epidemiology of traumatic brain injury in europe: a living systematic review, J. Neurotrauma 38 (10) (2021 May) 1411–1440, https://doi.org/10.1089/neu.2015.4126. PMID: 26537996; PMCID: PMC8082737.

[2] G.F. Miller, J. Daugherty, D. Waltzman, K. Sarmiento, Predictors of traumatic brain injury morbidity and mortality: examination of data from the national trauma data bank: predictors of TBI morbidity & mortality, Injury 52 (5) (2021 May) 1138–1144, https://doi.org/10.1016/j.injury.2021.01.042. PMID: 33551263; PMCID: PMC8107124.

[3] L. Chang, Y. Guo, X. Huang, et al., Experimental study on the protective performance of bulletproof plate and padding materials under ballistic impact, Mater. Des. 207 (2021) 109841, https://doi.org/10.1016/j.matdes.2021.109841.

[4] M.C. Dewan, A. Rattani, S. Gupta, et al., Estimating the global incidence of traumatic brain injury, J. Neurosurg. 130 (4) (2018 Apr) 1080–1097, https://doi.org/10.3171/2017.10.jns17352. PMID: 29701556.

[5] A.I.R. Maas, D.K. Menon, P.D. Adelson, et al., Traumatic brain injury: integrated approaches to improve prevention, clinical care, and research, Lancet Neurol. 16 (12) (2017 Dec) 987–1048, https://doi.org/10.1016/s1474-4422(17)30371-x. PMID: 29122524.

[6] M. Punchak, J. Abdelgadir, O. Obiga, et al., Mechanism of pediatric traumatic brain injury in southwestern Uganda: a prospective cohort of 100 patients, World Neurosurgery 114 (2018 Jun) e396–e402, https://doi.org/10.1016/j.wneu.2018.02.191. PMID: 29530703.

[7] D. Sanchez-Molina, J. Velazquez-Ameijide, C. Arregui-Dalmases, J.R. Crandall, C.D. Untaroiu, Minimization of analytical injury metrics for head impact injuries, Traffic Inj. Prev. 13 (2012) 278–285, https://doi.org/10.1080/15389588.2011.650803. PMID: 22607250.

[8] F.A. Fernandes, R.J. de Sousa, Head injury predictors in sports trauma–a state-of-the-art review, Proc. Inst. Mech. Eng. H 229 (8) (2015 Aug) 592–608, https://doi.org/10.1177/0954411915592906. PMID: 26238791.

[9] B. Hoshizaki, A. Post, M. Kendall, C. Karton, S. Brien, The relationship between head impact characteristics and brain trauma, J. Neurol. Neurophysiol. 5 (2013) 181, https://doi.org/10.4172/2155-9562.1000181.

[10] A.A. Ladak, S.A. Enam, M.T. Ibrahim, A review of the molecular mechanisms of traumatic brain injury, World Neurosurgery 131 (2019 Nov) 126–132, https://doi.org/10.1016/j.wneu.2019.07.039. PMID: 31301445.

[11] H. Abdi, K. Hassani, S. Shojaei, An investigation of the effect of brain atrophy on brain injury in multiple sclerosis, J. Theor. Biol. 557 (2023 Jan) 111339, https://doi.org/10.1016/j.jtbi.2022.111339. PMID: 36335998.

[12] H. Abdi, K. Hassani, S. Shojaei, An investigation of cerebral bridging veins rupture due to head trauma, Comput. Methods Biomech. Biomed. Eng. 26 (7) (2023 May) 854–863, https://doi.org/10.1080/10255842.2022.2092728. PMID: 35754388.

[13] S. Chatelin, A. Constantinesco, R. Willinger, Fifty years of brain tissue mechanical testing: from in vitro to in vivo investigations, Biorheology 47 (5–6) (2010) 255–276, https://doi.org/10.3233/bir-2010-0576. PMID: 21403381.

[14] D. Sánchez-Molina, C. Arregui-Dalmases, J. Velázquez-Ameijide, M. Angelini, J. Kerrigan, J. Crandall, Traumatic brain injury in pedestrian-vehicle collisions: convexity and suitability of some functionals used as injury metrics, Comput Methods Programs Biomed 136 (2016 Nov) 55–64, https://doi.org/10.1016/j.cmpb.2016.08.007. Epub 2016 Aug 20. PMID: 27686703.

[15] David B. MacManus, Mazdak Ghajari, Material properties of human brain tissue suitable for modelling traumatic brain injury, rain Multiphysics (2022) 100059, https://doi.org/10.1016/j.brain.2022.100059.

[16] S. Kleiven, Influence of impact direction on the human head in prediction of subdural hematoma, J. Neurotrauma 20 (4) (2003 Apr) 365–379, https://doi.org/10.1089/089771503765172327. PMID: 12866816.

[17] J.M.C. Costa, F.A.O. Fernandes, R.J. Alves de Sousa, Prediction of subdural haematoma based on a detailed numerical model of the cerebral bridging veins, J. Mech. Behav. Biomed. Mater. 111 (2020 Nov) 103976, https://doi.org/10.1016/j.jmbbm.2020.103976. Epub 2020 Jul 28. PMID: 32750673.

[18] J.A. van Dommelen, T.P. van der Sande, M. Hrapko, G.W. Peters, Mechanical properties of brain tissue by indentation: interregional variation, J. Mech. Behav. Biomed. Mater. 3 (2) (2010 Feb) 158–166, https://doi.org/10.1016/j.jmbbm.2009.09.001. PMID: 20129415.

[19] S. Kleiven, Why most traumatic brain injuries are not caused by linear acceleration but skull fractures are, Front. Bioeng. Biotechnol. 1 (2013) 15, https://doi.org/10.3389/fbioe.2013.00015. PMID: 25022321; PMCID: PMC4090913.

[20] S. García-Vilana, D. Sánchez-Molina, J. Velázquez-Ameijide, J. Llumà, Injury metrics for assessing the risk of acute subdural hematoma in traumatic events, Int J Environ Res Public Health 18 (24) (2021 Dec 17) 13296, https://doi.org/10.3390/ijerph182413296. PMID: 34948905; PMCID: PMC8702226.

[21] L. Zhang, K.H. Yang, R. Dwarampudi, et al., Recent advances in brain injury research: a new human head model development and validation, Stapp car Crash Journal 45 (2001 Nov) 369–394, https://doi.org/10.4271/2001-22-0017. PMID: 17458754.

[22] S. Kleiven, Predictors for traumatic brain injuries evaluated through accident reconstructions, Stapp car Crash Journal 51 (2007 Oct) 81–114, https://doi.org/10.4271/2007-22-0003. PMID: 18278592.

[23] T.J. Horgan, M.D. Gilchrist, The creation of three-dimensional finite element models for simulating head impact biomechanics, Int. J. Crashworthiness 8 (2003) 353–366, https://doi.org/10.1533/ijcr.2003.0243.

[24] B. Yang, K.M. Tse, N. Chen, et al., Development of a finite element head model for the study of impact head injury, BioMed Res. Int. 2014 (2014) 408278, https://doi.org/10.1155/2014/408278. PMID: 25405201; PMCID: PMC4227498.

[25] W. Zhao, S. Ji, Displacement- and strain-based discrimination of head injury models across a wide range of blunt conditions, Ann. Biomed. Eng. 48 (6) (2020 Jun) 1661–1677, https://doi.org/10.1007/s10439-020-02496-y. PMID: 32240424; PMCID: PMC7286792.

[26] F.A. Fernandes, D. Tchepel, R.J.A. de Sousa, M. Ptak, Development and validation of a new finite element human head model: yet another head model (YEAHM), Eng. Comput. 35 (2018) 477–496, https://doi.org/10.1108/EC-09-2016-0321.

[27] X. Li, Z. Zhou, S. Kleiven, An anatomically detailed and personalizable head injury model: significance of brain and white matter tract morphological variability on strain, Biomech. Model. Mechanobiol. 20 (2) (2021 Apr) 403–431, https://doi.org/10.1007/s10237-020-01391-8. PMID: 33037509; PMCID: PMC7979680.

[28] X. Huang, Q. Zheng, L. Chang, Z. Cai, Study on protective performance and gradient optimization of helmet foam liner under bullet impact, Sci. Rep. 12 (1) (2022 Sep 26) 16061, https://doi.org/10.1038/s41598-022-20533-9. PMID: 36163460; PMCID: PMC9512778.

[29] P. Dixit, G.R. Liu, A review on recent development of finite element models for head injury simulations, Arch Computat Methods Eng 24 (2017) 979–1031, https://doi.org/10.1007/s11831-016-9196-x.

[30] D. Sánchez-Molina, S. García-Vilana, J. Llumà, I. Galtés, J. Velázquez-Ameijide, M.C. Rebollo-Soria, C. Arregui-Dalmases, Mechanical behavior of blood vessels: elastic and viscoelastic contributions, Biology 10 (9) (2021 Aug 26) 831, https://doi.org/10.3390/biology10090831. PMID: 34571709; PMCID: PMC8472519.

[31] N. Famaey, Z. Ying Cui, G. Umuhire Musigazi, J. Ivens, B. Depreitere, E. Verbeken, J. Vander Sloten, Structural and mechanical characterisation of bridging veins: a review, J. Mech. Behav. Biomed. Mater. 41 (2015 Jan) 222–240, https://doi.org/10.1016/j.jmbbm.2014.06.009. Epub 2014 Jul 11. PMID: 25052244.

[32] Ming Tse Kwong, Siak Piang Lim, Vincent Beng Chye Tan, Heow Pueh Lee, A review of head injury and finite element head models, American Journal of Engineering, Technology and Society 1 (5) (2014) 28–52.

[33] S. García-Vilana, D. Sánchez-Molina, J. Llumà, I. Galtés, J. Velázquez-Ameijide, M.C. Rebollo-Soria, C. Arregui-Dalmases, Viscoelastic characterization of parasagittal bridging veins and implications for traumatic brain injury: a pilot study, Bioengineering (Basel) 8 (10) (2021 Oct 18) 145, https://doi.org/10.3390/bioengineering8100145. PMID: 34677218; PMCID: PMC8533420.

[34] S. Budday, T.C. Ovaert, G.A. Holzapfel, et al., Fifty shades of brain: a review on the mechanical testing and modeling of brain tissue, Arch Computat Methods Eng 27 (2020) 1187–1230, https://doi.org/10.1007/s11831-019-09352-w.
[35] Y. Feng, E.H. Clayton, Y. Chang, R.J. Okamoto, P.V. Bayly, Viscoelastic properties of the ferret brain measured in vivo at multiple frequencies by magnetic resonance elastography, J. Biomech. 46 (5) (2013 Mar) 863–870, https://doi.org/10.1016/j.jbiomech.2012.12.024. PMID: 23352648; PMCID: PMC3616770.
[36] K.J. Streitberger, E. Wiener, J. Hoffmann, et al., In vivo viscoelastic properties of the brain in normal pressure hydrocephalus, NMR Biomed. 24 (4) (2011 May) 385–392, https://doi.org/10.1002/nbm.1602. PMID: 20931563.
[37] L. Zhang, K.H. Yang, A.I. King, Comparison of brain responses between frontal and lateral impacts by finite element modeling, J. Neurotrauma 18 (1) (2001 Jan) 21–30, https://doi.org/10.1089/089771501750055749. PMID: 11200247.
[38] T.J. Horgan, M.D. Gilchrist, Influence of FE model variability in predicting brain motion and intracranial pressure changes in head impact simulations, Int. J. Crashworthiness 9 (4) (2004 Aug 1) 401–418, https://doi.org/10.1533/ijcr.2004.0299.
[39] W. Yan, O.D. Pangestu, A modified human head model for the study of impact head injury, Comput. Methods Biomech. Biomed. Eng. 14 (12) (2011 Dec) 1049–1057, https://doi.org/10.1080/10255842.2010.506435. PMID: 21264785.
[40] R. Willinger, H.S. Kang, B. Diaw, Three-dimensional human head finite-element model validation against two experimental impacts, Ann. Biomed. Eng. 27 (3) (1999 May-Jun) 403–410, https://doi.org/10.1114/1.165. PMID: 10374732.
[41] M. Zoghi-Moghadam, A.M. Sadegh, Global/local head models to analyse cerebral blood vessel rupture leading to ASDH and SAH, Comput. Methods Biomech. Biomed. Eng. 12 (1) (2009 Feb) 1–12, https://doi.org/10.1080/10255840903064897. PMID: 18821190.
[42] Y. Chen, M. Ostoja-Starzewski, MRI-based finite element modeling of head trauma: spherically focusing shear waves, Acta Mech. 213 (2010) 155–167, https://doi.org/10.1007/s00707-009-0274-0.
[43] H. Abdi, D. Sanchez-Molina, S. Garcia-Vilana, V. Rahimi-Movaghar, Quantifying the effect of cerebral atrophy on head injury risk in elderly individuals: insights from computational biomechanics and experimental analysis of bridging veins, Injury (2023 Oct) 111125, https://doi.org/10.1016/j.injury.2023.111125. PMID: 37867025.
[44] Z.Y. Cui, N. Famaey, B. Depreitere, et al., On the assessment of bridging vein rupture associated acute subdural hematoma through finite element analysis, Comput. Methods Biomech. Biomed. Eng. 20 (5) (2017 Apr) 530–539, https://doi.org/10.1080/10255842.2016.1255942. PMID: 27838925.